Appl. Phys. B 74, 267–271 (2002)
DOI: 10.1007/s003400100783

Applied Physics B
Lasers and Optics

N. MIRCHIN[1,✉]
A. PELED[1]
Y. DROR[2,*]

Bleaching processes and their reaction rates in photo-excited chlorophyll solutions

[1] Electronics Department, Holon Academic Institute of Technology, 52 Golomb Street, Holon 58 102, Israel
[2] Biochemistry Department, Agricultural Faculty, Hebrew University, Rehovot 76 100, Israel

Received: 3 July 2001/Revised version: 19 November 2001
Published online: 7 February 2002 •

ABSTRACT Photo-bleaching phenomena occurring in chlorophyll-a were analysed by irradiation with UV and visible-spectrum sources. A mathematical formalism was developed to quantify the optical spatio-temporal properties of the irradiated solutions. We also measured the spatio-temporal changes of the optical response in photo-excited solutions. An empirical expression for the reaction rate was obtained and the model used to quantify and understand the experimental bleaching results.

PACS 82.50.N; 42.70.G

1 Introduction

Photo-excitation effects of inorganic colloid materials have been investigated previously in hydrosols [1–6] for developing various materials-processing methods. The basic processes observed during photonic excitation were the destabilisation of inorganic chromophores in liquid systems, which led to various phenomena such as photo-precipitation, volume photo-aggregation and surface photo-adsorption phenomena. Recently, photo-excited processes in bio-organic materials dispersed in liquid media also became of interest for possible new optical and optoelectronic technological applications [7, 8] by embedding chromophores in various matrices for non-linear optical properties. The purpose of this paper is to evaluate and understand the observed 'optical response' in experiments of photo-excited chlorophyll-a (chl-a) solutions [9].

2 Photo-bleaching phenomenological model

2.1 *Basic definition of the optical transmission parameters*

The photo-bleaching system is shown schematically in Fig. 1. One exciting photo-bleaching beam from an appropriate UV or visible-spectrum (VIS) light source propagates through the optical cell in the y direction. At the same time a He−Ne laser beam probes the cell along the x direction

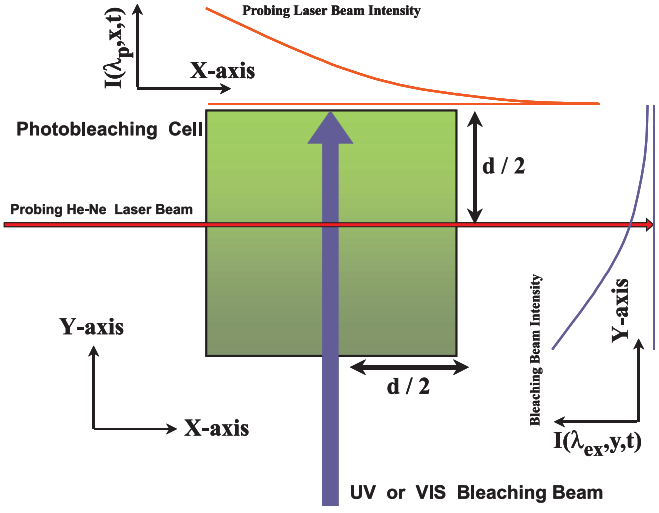

FIGURE 1 Schematic view of the photo-exciting and 'optical response' diagnostics system used to characterise the bleaching processes of the chl-a solution contained in a PMMA cuvette of Semadeni Corp., model 3893, suitable for UV and VIS transparency from about 280 to 800 nm. Typical absorbances were $OD(290\,\text{nm}) = 0.25$, $OD(350\,\text{nm}) = 0.05$, $OD(400\,\text{nm}) = 0.001$

without affecting the bleaching process since its wavelength is far from bond-disruptive photon energies.

The optical cell is a UV- and VIS-transparent cuvette with x-y square cross section of size d.

Following the designations used in Fig. 1, we realise that the exciting beam intensity $I_{\text{ex}}(\lambda_{\text{ex}}, y, t)$, which bleaches the solution, diminishes spatially along the y axis due to chlorophyll optical absorption at λ_{ex} but also changes in time and space due to chlorophyll bleaching. The bleaching rate however itself depends on the light-penetration depth along the y axis. Hence the non-bleached chromophore concentration in the cell, $N(x, y, z, t)$, has approximately only a y-dependent spatial dependence $N(y, t)$, being otherwise constant with respect to the other two spatial coordinates, i.e. x and z. The probing He−Ne beam has an intensity designated by $I_{\text{p}}(\lambda_{\text{p}}, x, t)$ that diminishes spatially due to non-bleaching light absorption in the x direction and it does not affect the chromophore concentration $N(\vec{r}, t) = N(x, y, z, t)$. The probing beam is hence used only for diagnosing the chromophore-concentration variation during the bleaching process.

✉ Fax: +972-3/502-6643, E-mail: mirchin@hait.ac.il
*Fax: +972-8/947-6189, E-mail: dror@agri.huji.ac.il

Using the space–time-dependent light-intensity function $I(\lambda, \vec{r}, t) = I(\lambda, x, y, z, t)$, one may write for convenience a vectorial equation describing the photon flux intensity change in any $x-y$ plane of the volume of the irradiated cell during the bleaching process. Specifically the incremental absorption of light $\overrightarrow{\mathrm{d}I} = \begin{bmatrix} \mathrm{d}I_{\mathrm{p}}(x) \\ \mathrm{d}I_{\mathrm{ex}}(y) \end{bmatrix}$ in an infinitesimal layer $\overrightarrow{\mathrm{d}l} = \begin{bmatrix} \mathrm{d}x \\ \mathrm{d}y \end{bmatrix}$ can be represented by a generalised 2D, vectorial Beer–Lambert law:

$$\overrightarrow{\mathrm{d}I} = N(x, y, z, t) \begin{bmatrix} \sigma_{\mathrm{p}}(\lambda_{\mathrm{p}})\,\mathrm{d}x \\ \sigma_{\mathrm{ex}}(\lambda_{\mathrm{ex}})\,\mathrm{d}y \end{bmatrix} \tag{1}$$

where $\vec{I}$ is the flux intensity in units of photons/(cm^{2}s) or W/(cm^{2}s) and $N(\vec{r}, t)$ is the chlorophyll molecular spatial concentration which depends on time due to bleaching, given typically in units of molecules/cm^3. $\vec{\sigma}(\lambda) = \begin{bmatrix} \sigma_{\mathrm{p}}(\lambda_{\mathrm{p}}) \\ \sigma_{\mathrm{ex}}(\lambda_{\mathrm{ex}}) \end{bmatrix}$ is the 2D cross-section vector composed of two components, i.e. optical non-bleaching $\sigma_{\mathrm{p}}(\lambda_{\mathrm{p}})$ and bleaching $\sigma_{\mathrm{ex}}(\lambda_{\mathrm{ex}})$ optical absorption cross sections, typically given in units of cm^2. The spatial vector $\overrightarrow{l} = (x, y)$ represents only formally the directions of the propagation of the two beams, i.e. x for the probing beam which measures the non-bleaching light-beam intensity $I_{\mathrm{p}}(x)$ and y for the exciting beam which bleaches the medium with a beam intensity $I_{\mathrm{ex}}(y)$.

These vectorial parameters can also be related for convenience to a 2D-generalised vectorial optical absorption coefficient $\overrightarrow{\alpha}$ of the medium:

$$\overrightarrow{\alpha}(\lambda, x, y, z, t) = \overrightarrow{\sigma}(\lambda) N(x, y, z, t) \tag{2}$$

Since at the exciting wavelength λ_{ex} and the probing wavelength λ_{p} we have two different optical attenuation mechanisms, we have also two different optical absorption constants, one, α_{ex}, given by

$$\alpha_{\mathrm{ex}}(\lambda_{\mathrm{ex}}, x, y, z, t) = \sigma_{\mathrm{ex}}(\lambda_{\mathrm{ex}}) N(x, y, z, t) \tag{3}$$

which relates to a bleaching optical absorption coefficient of the chromophores, and the other, an optical absorption coefficient due to non-bleaching effects α_{p} given by

$$\alpha_{\mathrm{p}}(\lambda_{\mathrm{p}}, x, y, z, t) = \sigma_{\mathrm{p}}(\lambda_{\mathrm{p}}) N(x, y, z, t) \tag{4}$$

The full explicit vectorial designation of $\overrightarrow{\sigma}$ is hence given by

$$\overrightarrow{\alpha} = \begin{bmatrix} \alpha_{\mathrm{p}}(\lambda_{\mathrm{p}}, x, y, t) \\ \alpha_{\mathrm{ex}}(\lambda_{\mathrm{ex}}, x, y, z, t) \end{bmatrix} = \begin{bmatrix} \sigma_{\mathrm{p}}(\lambda_{\mathrm{p}}) \\ \sigma_{\mathrm{ex}}(\lambda_{\mathrm{ex}}) \end{bmatrix} N(x, y, z, t)$$

Experimentally we measure during UV or VIS light excitation (and for some time after it is stopped) the temporal optical transmission of the solution in the cell of optical path d by a laser probing beam, i.e. $I_{\mathrm{p}}(x = d)$. The corresponding optical absorbance correlates to a first approximation (while neglecting effects such as turbulence and convection) to the concentration of the chromophores at a plane defined by $y = d/2$ in the cell. The probing optical transmission is defined as the ratio of transmitted light intensity through the cell in the x direction at a plane defined by $y = d/2$, i.e., $I^{\mathrm{p}}_{\mathrm{tr}}(x = d, y = d/2)$ to the incident probing light intensity $I^{\mathrm{p}}_0(x = 0, y = d/2)$. The transmission parameter, $T_{\mathrm{p}} = I^{\mathrm{p}}_{\mathrm{tr}}/I^{\mathrm{p}}_0$, can be used to evaluate the time variation of the probing beam optical absorption coefficient of the chlorophyll solution at λ_{p} given by

$$\alpha_{\mathrm{p}}(t) = \frac{1}{d} \ln\left(\frac{1}{T_{\mathrm{p}}(x = d, y = d/2, t)}\right) \tag{5}$$

2.2 *Optical time-dependent transmission theory of chlorophyll bleaching*

We develop here a simple formalism for the photobleaching process in the solutions. The irradiated zone close to the cell entrance window becomes highly photo-excited, obstructing the penetration of the radiation into the bulk of the photo-reactor. The beam intensities $I_{\mathrm{ex}}(\lambda_{\mathrm{ex}}, y, t)$ and $I_{\mathrm{p}}(\lambda_{\mathrm{p}}, x, t)$ in the cell in the x and y directions can be obtained by integrating (1) along x and y coordinates respectively.

The generalised vectorial transmission function $\overrightarrow{T(x, y)}$ depending on x and y is given by

$$\overrightarrow{T(x, y)} = \begin{bmatrix} T_{\mathrm{p}} \\ T_{\mathrm{ex}} \end{bmatrix} = \begin{bmatrix} I_{\mathrm{p}}(x)/I_{\mathrm{p}}(0) \\ I_{\mathrm{ex}}(y)/I_{\mathrm{ex}}(0) \end{bmatrix} = \begin{bmatrix} \exp\left(-\int_0^x \sigma_{\mathrm{p}} N \mathrm{d}x\right) \\ \exp\left(-\int_0^y \sigma_{\mathrm{ex}} N \mathrm{d}y\right) \end{bmatrix} \tag{6}$$

Using now the following relation between $\overrightarrow{\alpha}$ and $\overrightarrow{T}$:

$$\overrightarrow{\alpha} = -\ln \overrightarrow{T}$$

we obtain from (6) an equation useful for observing the temporal dependence of N from the time evolution of the transmission function $\overrightarrow{T}$:

$$\overrightarrow{\sigma} \cdot N(t) = -\ln \overrightarrow{T}(t) \tag{7}$$

Finally, we can assume as an approximation that both the bleaching beam intensity $I_{\mathrm{ex}}(\lambda_{\mathrm{ex}}, y, t)$ and the concentration of the chromophores $N(x, y, z, t)$ are homogenous in the x direction, since optical excitation occurs mainly in the y direction (when scattering effects are negligible). This gives after spatial integration of the probing transmission function in (7), from $x = 0$ to $x = d$, the following result:

$$N(\lambda_{\mathrm{p}}, y, t) = -\frac{1}{\sigma_{\mathrm{p}} d} \ln T_{\mathrm{p}}(t) \tag{8}$$

$T_{\mathrm{p}}(t)$ is the experimentally measured transmission of the non-bleaching laser probing optical beam with wavelength λ_{p} at $x = d$ and time t, i.e. $T_{\mathrm{p}}(t) = T_{\mathrm{p}}(y = d/2, x = d, \lambda_{\mathrm{p}}, t)$.

2.3 *Photo-bleaching reaction-rate formalism*

The photo-bleaching rate function $R(t)$ for chromophore depletion is obtained by time derivation of (8):

$$R = \frac{\mathrm{d}N(\lambda_{\mathrm{p}}, y, t)}{\mathrm{d}t} = -\frac{1}{\sigma_{\mathrm{p}} d} \frac{d}{\mathrm{d}t}\left(\ln T_{\mathrm{p}}(t)\right) = -\frac{1}{\sigma_{\mathrm{p}} \mathrm{d}T_{\mathrm{p}}} \frac{\mathrm{d}T_{\mathrm{p}}}{\mathrm{d}t} \tag{9}$$

Hence $N(\lambda_p, x = d/2, y, t)$ is calculable from the probing beam transmission function $T_p(t)$. Analysing the chromophore concentration $N(t)$ as a function of time may be subsequently used from (8) and (9) to suggest possible mechanisms for the photo-bleaching.

3 Experimental

The samples for the photo-bleaching experiments were prepared by extracting chlorophyll-a from Senecio Mikanioides (Parlor Ivy) leaves by cell suspension and solvation in 95% ethanol as explained in detail in [9]. Photo-excitation experiments of the chlorophyll solutions by sources of ultraviolet and visible-spectrum bands along the y axis were performed with simultaneous perpendicular optical transmission probing along the x direction of a He−Ne beam, $\lambda = 633$ (nm), in 1-cm-optical path cuvettes (Semadeni Co., type 3893) made of highly transparent polymethylmethacrylate (PMMA) [9]. The setup for photo-excitation and simultaneous orthogonal probing with the He–Ne laser beam is given in Fig. 1. VIS irradiation from a tungsten–halogen incandescent lamp with optical fibre guiding was used for excitation; its spectrum is given in the inset of Fig. 2 and its electrical characteristics in the caption. Also, a UV source, a polymer-curing illuminator (Dr. Höhnle), was used whose characteristics are given in the caption of Fig. 3 and the spectrum shown in the inset. The irradiated samples were aliquots of 4 ml introduced into the PMMA cuvettes. The cuvette's walls were transparent in the whole spectrum band of 280–800 nm, i.e. with an absorbance OD less than $OD = log(T^{-1}) = 0.25$ at $\lambda = 290$ (nm) and lower than $OD = 0.001$ from $\lambda = 400$ (nm) and up, throughout the whole visible spectrum. When irradiated with broad-band light sources of short wavelength, $\lambda < 400$ (nm), the solutions became excited by UV and VIS sources in such a way that the chlorophyll solution was bleached during typical times of minutes. The bleaching effects were monitored in situ by optical transmission measurements using a He−Ne laser beam (2 mW, $\lambda = 633$ nm, 2 mm cross-beam diameter) perpendicular to the photo-exciting source beam to follow the kinetics of the photo-bleaching for the two broad-band sources. It is important to note that the He−Ne beam did not bleach the chl-a solutions and was very useful therefore for probing the solution optical properties.

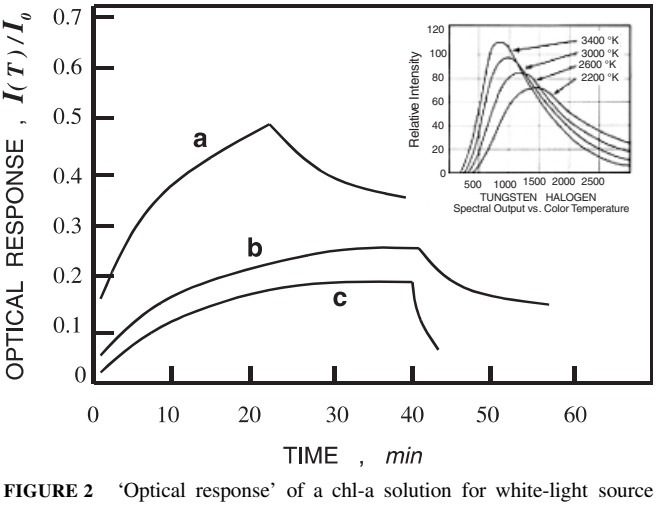

FIGURE 2 'Optical response' of a chl-a solution for white-light source irradiation: (a) I_0 without UV filtering; (b) I_0 with UV removal by glass-window filtering; (c) $0.5I_0$ with UV removal by glass-window filtering; the source was a GE-Thorn quartz–halogen–tungsten lamp, model DDL. Its maximum electrical rating at 20 V was 150 W, through a fibre illuminator type Volpi AG, supplying an integrated light intensity of about $I_0 = 0.375$ W/cm^2 in the spectral region 300–400 nm and $I_0 = 3.75$ W/cm^2 in the visible region 400–800 nm at the fibre tip. The spectrum of this lamp is continuous, black-body type and used typically with a maximum colour temperature of about 3400 K. The inset shows the typical spectrum of tungsten–halogen lamps as a function of colour temperature

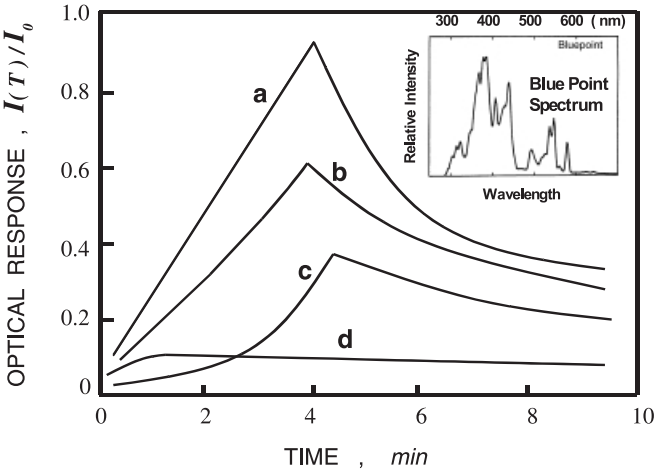

FIGURE 3 'Optical response' of chl-a solution for UV light source irradiation; intensities were varied by changing only the areas of the irradiating beam. (a) I_0; (b) $0.25I_0$; (c) $0.05I_0$; (d) $0.015I_0$; the UV radiation was supplied by a Dr. Höhnle Co. polymer-curing fibre illuminator, type 'Blue Point', with a maximum intensity of $I_0 = 1.45$ W/cm^2 in the UV band 290–390 nm. The lamp was driven with an overall maximum electrical power of 300 W. The inset shows the typical spectrum of the UV lamp

Figures 2 and 3 show respectively typical time-dependent 'optical responses' in terms of the probing laser beam optical transmission during the simultaneous transverse VIS or UV light-source excitation of the solutions and after the irradiation is stopped for various light intensities. To avoid spectral shifts of the illuminating sources we have changed the intensities only geometrically by varying the distance of the illuminators' fibre tips from the optical cells while keeping the electrical driving parameters constant in all experiments. The parametric details are given in the Figs. 2 and 3 captions. Figure 2 illustrates the influence of the VIS source excitation for three light-intensity levels, where curve (a) is for a UV unfiltered tungsten–halogen lamp with VIS broad-band illumination spectra (Thorn-GE lamp, model DDL) and curve (b) and curve (c) are with simple glass UV filtering.

Using UV broad-band source irradiation (Dr. Höhnle Co., polymer curing lamp, model: Blue Point) we obtained a different behaviour for the rising part of the probing transmission curves ('optical response'), in the range of light intensities used, as seen in Fig. 3.

Specifically, we observe for the VIS source irradiation an 'under-linear' time-dependent rising behaviour of the 'optical response' curve while, for UV source irradiation, the 'optical response' curves show a 'supra-linear' or 'quasi-linear' time behaviour. The 'linearity' or 'non-linearity' concepts refer here only to the sloping shape of the rising parts of the probing transmission as a function of time, i.e. $T(t)$.

3.1 *Fitting the experimental data to the model formalism*

We tried to fit the experimental data in the rising part of the transmission response curves in Figs. 2 and 3, i.e. during the 'on'-time of irradiation, to the following set of experimental–phenomenological time-dependent functions [9]:

$$T_{\mathrm{p}}(t) = at^{n} \quad \text{with} \quad n > 1 \quad \text{or} \quad n < 1 \tag{10}$$

where t denotes time, and a and n are fitting constants where n is non-dimensional and the dimensions of a are $[a] = [t]^{-n}$.

The results of the fitting obtained in [9] showed for UV excitation $n \geq 1$ with $a < 0.25$ while for VIS excitation $n < 1$ with $a < 0.16$. Combining (9) and (10) we obtain for the photo-bleaching reaction rate the following time dependence:

$$R = \frac{n}{\sigma_{\mathrm{p}} dt} \tag{11}$$

Using the optical transmission dependence on the concentration of the non-bleached chlorophyll chromophores given in (7) and observing from (10) that $t = \left(T_{\mathrm{p}}/a\right)^{1/n}$, we obtain from (11) the following reaction-rate equation:

$$R = \frac{n}{\sigma_{\mathrm{p}} d} \left(\frac{a}{T_{\mathrm{p}}}\right)^{1/n} \tag{12}$$

Finally, using (5) to eliminate T_{p} in (12) we obtain a simple model equation for the photo-bleaching:

$$R = \frac{n a^{1/n}}{\sigma_{\mathrm{p}} d} \exp\left(\frac{\sigma_{\mathrm{p}} N d}{n}\right)$$

The calculated bleaching reaction rates of the chlorophyll for different irradiation intensities and wavelengths obtained using $T_{\mathrm{p}}(t) = T_{\mathrm{p}}(y = \frac{d}{2}, x = d, \lambda_{\mathrm{p}}, t)$ in (12) are given in Tables 1 and 2.

Here $k = d/n$ and $\zeta = (na^{1/n}/d)$ are new defined parameters with some physical insight. k is the exciting beam characteristic penetrating depth into the solution and ζ is a characteristic photo-bleaching rate per unit distance.

$R_{\mathrm{vis}}(t) = \frac{\zeta}{\sigma_{\mathrm{p}}} \exp\left(k\sigma_{\mathrm{p}} N\right)$	ζ $\mathrm{cm}^{-1}\mathrm{sec}^{-1}$	k cm
a	0.0022	2.78
b	0.0003	2.60
c	0.0006	2.0

TABLE 1 Photo-bleaching rate for VIS excitation for the curves (a)–(c) in Fig. 2

$R_{\mathrm{UV}}(t) = \frac{\zeta}{\sigma_{\mathrm{p}}} \exp\left(k\sigma_{\mathrm{p}} N\right)$	ζ $\mathrm{cm}^{-1}\mathrm{sec}^{-1}$	k cm
a	0.204	1.08
b	0.141	1.02
c	0.275	0.45

TABLE 2 Photo-bleaching rate for UV light excitation for the curves (a)–(c) in Fig. 3

The general trend observed in Tables 1 and 2 is that the higher the exciting beam intensity, the greater the penetration depth k of the beam and the higher the photo-bleaching rate ζ. We also observe that ζ is at least two orders of magnitude higher for the UV source excitation as compared to the VIS source excitation. The penetration depth, k, however, differs only by a factor of 2–3 for the two cases.

4 Discussion

In this section we derive the photo-bleaching time behaviour of the chlorophyll concentration from the proposed model. Then we calculate and discuss the chromophore optical cross sections and half lifetimes of the photo-bleaching processes from combining theory and experimental data.

Using (9) and (11) one obtains the following relation for the photo-bleaching rate of the chromophores:

$$-\frac{dN}{dt} = \beta t^{-1} \tag{13}$$

where the parameter β is defined by

$$\beta\left(I_{\mathrm{ex}_0}(x=0), \lambda_{\mathrm{ex}}, \sigma_{\mathrm{p}}\right) = \frac{n\left(I_{\mathrm{ex}_0}, \lambda_{\mathrm{ex}}\right)}{\sigma_{\mathrm{p}} d} \tag{14}$$

and I_{ex_0} is the intensity of the photo-bleaching irradiation penetrating the cell at the plane defined by

$$x = 0\,.$$

Integrating (13) with the initial concentration value $N = N_0$ at $t = t_0$ we obtain

$$N = N_0 - \beta \ln\left(t t_0^{-1}\right) \tag{15}$$

The initial chlorophyll concentration at $t = t_0$ calculated from spectroscopic analysis was about $N_0 = 4$ ($\mu\mathrm{g/cm}^3$) or $N_0 = 2.7 \times 10^{15}$ (molecules/cm^3).

Using (15) one may define a photo-bleaching reaction half-life time, $t_{1/2}$, i.e. the time it takes the initial chlorophyll concentration to decay to half its initial value, i.e. $N\left(t_{1/2}\right) = \frac{N_0}{2} = \frac{N_{\max}}{2}$. From (15) we hence realise that the non-bleached chlorophyll concentration at $t_{1/2}$ is given by

$$N_{1/2} = N\left(t_{1/2}\right) = N_0 - \beta \ln\left(t_{1/2} t_0^{-1}\right) = N_0/2 \tag{16}$$

with

$$N_0 = 2\beta \ln\left(t_{1/2} t_0^{-1}\right)\,.$$

This characteristic time, $t_{1/2}$, for photo-bleaching, corresponds to a specific experimental transmission $T_{\mathrm{p}_{1/2}}$ while a maximum transmission value $T_{\mathrm{p}_{\max}}$ corresponds to a characteristic time $t_{\max}$ for which the chromophore concentration is down to $N\left(t_{\max}\right) = N\left(T_{\mathrm{p}_{\max}}\right) = N_{\min}$. Thus we obtain from (15) the following specific characteristic transmission values:

$$T_{\mathrm{p}_{1/2}} = \mathrm{e}^{-2\sigma_{\mathrm{p}} N_{\min} d} \quad \text{and} \quad T_{\mathrm{p}_{\max}} = \mathrm{e}^{-\sigma_{\mathrm{p}} N_{\min} d}$$

Using the above expressions for the VIS and UV excitations we obtain from Figs. 2 and 3 the time constants given in Tables 3 and 4.

Curve	t_{max} min	T_{pmax}	$T_{p1/2}$	$t_{1/2}$ min
a	21	0.51	0.25	3.60
b	40	0.25	0.06	2.40
c	40	0.20	0.04	2.45

TABLE 3 Calculated half-life times $t_{1/2}$ and t_{max} for the VIS excitation experiments

Curve	t_{max} min	T_{pmax}	$T_{p1/2}$	$t_{1/2}$ min
a	4.0	0.91	0.81	3.55
b	3.9	0.60	0.36	2.45
c	4.0	0.28	0.078	2.35

TABLE 4 Calculated half-life times $t_{1/2}$ and t_{max} for the UV excitation experiments

Curve	n	$t_{1/2}$ min	$\sigma_p \times 10^{-16}$ $cm^2(t_0 = 10^{-5}$ min)	$\sigma_p \times 10^{-16}$ $cm^2(t_0 = 10^{-15}$ min)
a	0.36	3.60	3.412	9.55
b	0.38	2.40	3.487	9.97
c	0.49	2.45	4.504	12.86

TABLE 5 Photo-bleaching cross sections for the VIS light excitation experiments

Curve	n	$t_{1/2}$ min	$\sigma_p \times 10^{-16}$ $cm^2(t_0 = 10^{-5}$ min)	$\sigma_p \times 10^{-16}$ $cm^2(t_0 = 10^{-15}$ min)
a	0.92	3.55	8.71	24.40
b	0.98	2.45	9.01	25.72
c	2.21	2.35	20.25	57.94

TABLE 6 Photo-bleaching cross sections for the UV excitation experiments

Surprisingly we observe from the tables that the reaction half-life time, $t_{1/2}$, has only a small variation, i.e. 2–4 min for both VIS and UV excitation while t_{max} differs by a factor of 5–10 (4–40 min). We also observe from Table 2 for the UV-filtered VIS source a relatively small bleaching rate difference in the curves (b) and (c) as compared to curve (a), which is non-UV-filtered, see also Fig. 2. Both results suggest that the bleaching reaction is caused only by energetic UV photons, and that the slight differences in the half-life time for UV vs. VIS source excitation is due only to secondary influences such as irradiation intensity. We also observe an approximate linear dependence for the half-life time vs. the intensity of irradiation for the UV case, i.e. $t_{1/2} \sim I_{UV}$, which means that the photo-bleaching process is directly dose-dependent and possesses a memory-like effect for the amount of non-bleached material retained in the reactor at any time after irradiation stops.

From β given in (14) and (16) we may also obtain an estimation for the chromophore optical cross section:

$$\sigma_p = \frac{2n}{N_0 d} \ln\left(t_{1/2} t_0^{-1}\right) \tag{17}$$

The calculated values of σ_p are given in Tables 5 and 6 for two short but arbitrary values of initial times $t_0 = 10 \times 10^{-5}$ min and $t_0 = 10 \times 10^{-15}$ min.

From these tables we observe that the optical cross sections for the two cases, i.e. UV and VIS, are very similar in magnitude, i.e. in the range $3-13 \times 10^{-16}\,cm^{-2}$ for the VIS and $8-58 \times 10^{-16}\,cm^{-2}$ for the UV. This typical value strengthens again the hypothesis that in both cases it is the UV photons which are responsible for the bleaching effect. These optical cross sections are also very similar in magnitude to cross sections of other photo-chromic organic materials such as azo dyes and pseudo-stylbene molecules [8] investigated for photonic non-linear applications.

5 Conclusions

We found in this investigation that the half-life time $t_{1/2}$ for the bleaching reaction in the chlorophyll solution is almost identical for the UV and VIS irradiation, i.e. in the range 2–4 min, suggesting a UV-based photo-bleaching of the chlorophyll material that is dose-dependent.

The reaction time period t_{max} that it takes to reach the maximum amount of bleached molecules in the experiments is fast for the UV broad-band illuminator case (≈ 4 min) as compared to slow (40 min) for the VIS tungsten–halogen-source excitation. Chlorophyll is therefore bleached much faster by using the UV broad-band spectral source due to the abundance of UV photons as compared to the low content of UV photons of the broad-band VIS source. Using a simple model formalism developed in this work we found that the time-dependent optical cross sections of the bleaching chromophores were in the range of $3-18 \times 10^{-16}\,cm^{-2}$ for the VIS source and $8-58 \times 10^{-16}\,cm^{-2}$ for the UV irradiation source. This relatively small difference strengthens our conclusion that only the most energetic photons, i.e. UV photons, are responsible for photo-bleaching. These results open new ways for using spectral excitation variations in photonic reversible and permanent memory applications by realising that permanent memory writing can be achieved in these systems by UV photons while VIS photons have a more reversible-type excitation response.

ACKNOWLEDGEMENTS This work was supported in part by a grant obtained from the Israel Ministry of Immigration Absorption under Contract No. 280111934.

REFERENCES

1 A. Peled: Lasers Eng. **6**, 41 (1997)
2 V. Weiss, A.A. Friesem, A. Peled: J. Imaging Sci. Technol.**41**, 355 (1997)
3 A. Peled, B. Dragnea, R. Alexandrescu, A. Andrei: Appl. Surf. Sci. **86**, 538 (1995)
4 N. Borochov, A. Peled: Appl. Surf. Sci. **86**, 533 (1995)
5 N. Mirchin, A. Peled: Appl. Surf. Sci. **106**, 418 (1996)
6 A. Peled, Y. Dror: Opt. Eng. **27**, 482 (1988)
7 T. Okamoto, T. Fujiki, Y. Okada, I. Yamaguchi: Opt. Eng. **38**, 157 (1999)
8 D. Dantsker, S. Speiser: Appl. Phys. B **58**, 105 (1994)
9 A. Peled, Y. Dror, I. Baal-Zedaka, A. Porat, N. Mirchin, I. Lapsker: Synth. Metals **115**, 167 (2000)